Numerical simulations of temperature loads on multilayer Laue lenses

Z Rek[1], H N Chapman[2,3,4], S Bajt[3,4] and B Šarler[1,5]

[1] Laboratory for Fluid Dynamics and Thermodynamics, Faculty of Mechanical Engineering, University of Ljubljana, Aškerčeva 6, 1000 Ljubljana, Slovenia
[2] Department of Physics, Universität Hamburg, Luruper Chaussee 149, 22761 Hamburg, Germany
[3] Center for Free-Electron Laser Science CFEL, Deutsches Elektronen-Synchrotron DESY, Notkestr. 85, 22607 Hamburg, Germany
[4] The Hamburg Centre for Ultrafast Imaging, Luruper Chaussee 149, 22761 Hamburg, Germany
[5] Laboratory for Simulation of Materials and Processes, Institute of Metals and Technology, Lepi pot 11, 1000 Ljubljana, Slovenia

E-mail: bozidar.sarler@fs.uni-lj.si

Abstract. We present numerical simulations of the heat loads on novel diffractive X-ray optics, known as multilayer Laue lenses, exposed to high intensity X-ray beams produced by an X-ray free electron laser (XFEL). These lenses can be used to focus XFEL beams to nanometer spots. The temperature distribution within the lens and temperature change as a function of incident pulse frequencies were calculated for two different lens geometries and several material pairs and material ratios of the MLLs. Simulations took into account the special pulse structure of European XFEL with X-rays being delivered in pulse trains. After defining the geometric model, computational grid, material properties, and boundary conditions, a grid sensitivity study was carried out. We solved the transient heat energy transport equation in solids for mixed boundary conditions. Results of these simulations will help select materials and lens geometry for future XFEL experiments.

1. Introduction

Multilayer Laue lenses (MLLs) are novel diffractive X-ray optical elements that hold promise to focus X-rays to 1 nm [1]. They are usually used as lenses in X-ray microscopy for high resolution imaging at synchrotrons [2]. They are based on multilayer coatings and their diffraction efficiency generally increases with X-ray energy. They can also be used to focus X-ray free electron laser (XFEL) beams. These newly developed X-ray sources produce high intensity, coherent, and pulsed X-rays, which opened up new scientific investigations and applications spanning a wide range of disciplines. The intensity of unfocused XFEL beams is already many orders of magnitude higher than the intensity of the synchrotron beams since they compress the radiation into much shorter femtosecond pulses. However, some experiments, such as the imaging of weakly scattering objects (single particles or macromolecules) require even higher X-ray intensities. One way to achieve this is with extreme focusing, but this requires high quality X-ray optics such as MLLs.

The first experiment in which MLLs were used to focus XFEL beams was performed at the European XFEL facility [4]. These MLLs were based on tungsten carbide (WC) and silicon carbide (SiC) multilayers [6].They were prepared the same way as for synchrotron experiments but mounted on a diamond substrate instead on a Si substrate. At the European XFEL, X-rays are delivered in pulse trains spaced 100 ms apart (10 Hz), while the frequency of pulses inside the pulse trains can be as high as 4 MHz. However, most of the experiments are usually done with lower frequency (1–2 MHz). In the aforementioned experiment [4] the incident XFEL beam was pre-focused with compound refractive lenses to ~300 μm and additionally reduced with slits to 100 μm x 100 μm. This size matched the dimensions of MLLs. It was demonstrated that a pair of MLLs could be used for many hours with single XFEL pulses at 10 Hz frequency. However, when the MLLs were exposed to the pulse trains, each with more than 30 pulses at 0.25 MHz to 1 MHz pulse frequency, the lenses de-attached from the substrate. Since the X-rays have to diffract from the layers of the MLL to converge into a focus, the MLL has to be tilted to satisfy the Bragg angle. The diffraction efficiency depends on the materials in the MLLs as well as on the X-ray energy but part of the beam is always absorbed in the lens. Ideally, the portion of the absorbed beam is as small as possible. However, if the angle of the lens changes, such that the layers no longer match the Bragg angle, a greater portion of the X-rays are absorbed in the lens. As we mentioned above, MLLs have higher diffraction efficiency at higher X-ray energies. Since the European XFEL at the time of the experiment was not yet fully commissioned, the experiment had to be performed at relatively low energy (8.9 and 10.1 keV), which resulted in lower diffraction efficiency and higher absorbed dose in MLLs. This led to high thermal loads that caused the observed problems. Although WC/SiC multilayers have very high thermal stability, the high density WC material is not ideal due to its low damage threshold.

To better understand the heat transfer process and thermal loads in the MLLs we performed numerical simulations [7] since their complex geometry and boundary conditions preclude an analytical solution. This was done with ANSYS Fluent [8] software. Numerical simulations allowed us to quickly analyze the influence of boundary conditions, multilayer materials and their ratios in the lenses, as well as geometrical variations of the model under study.

We carried out several simulations to understand what caused de-attachment of the lenses and how to reduce heat load and increase heat transfer to the holder and the environment. Here, we present results of three studies. First, we compared the temperature distribution of two different lens geometries, the one used in European XFEL experiment and a new one with much larger contact between the lens and substrate holder. In the second study we investigated the effect of multilayer materials and their composition on the temperature distribution in the lens. Finally, we examined the effect of the X-ray pulse frequency on the temperature field inside the lens.

2. Numerical model

2.1. Governing equations and solution procedure

The equation which describes heat transfer in a solid body [9]**Error! Reference source not found.** is the diffusion equation

$$\frac{\partial}{\partial t}\left(\rho h\right) = \nabla \cdot \left(k \nabla T\right) + S_h, \tag{1}$$

where ρ is the density, h is the specific enthalpy, k is the thermal conductivity, T is the temperature, and S_h is the volumetric heat source. The enthalpy is calculated as

$$h = \int_{T_{\text{ref}}}^{T} c_p dT, \tag{2}$$

where c_p is the specific heat, and T_{ref} is the reference temperature. The solution of equation (1) for the prescribed boundary conditions gives the temperature field in the computational domain considered.

We used second-order implicit discretization for transient time formulation in the solution process. A maximum of 20 linear solver iterations were allowed in each time step. The spatial discretization for

the gradient operator was least-squares cell-based, while second-order spatial discretization was used for energy.

Because of the high frequency of the X-ray pulses, the calculation employed a special time step scheme. The size of the time step was 10^{-7} s during the period of the pulse triggering. After that, it was gradually changed to 10^{-6} s and finally to 10^{-3} s. The total simulation time was $t_{sim} = 0.1$ s, representing the time between two consecutive pulse trains. It was found that the steady-state temperature in the MLL was reached well before the next series of X-ray pulses arrived.

2.2. Geometric model and computational grid

The geometric model in figure 1 was assembled from three parts: lens, diamond plate, and aluminum holder. The MLL was mounted at the top-left position of the diamond plate (blue), which is attached to an aluminum holder (gray).

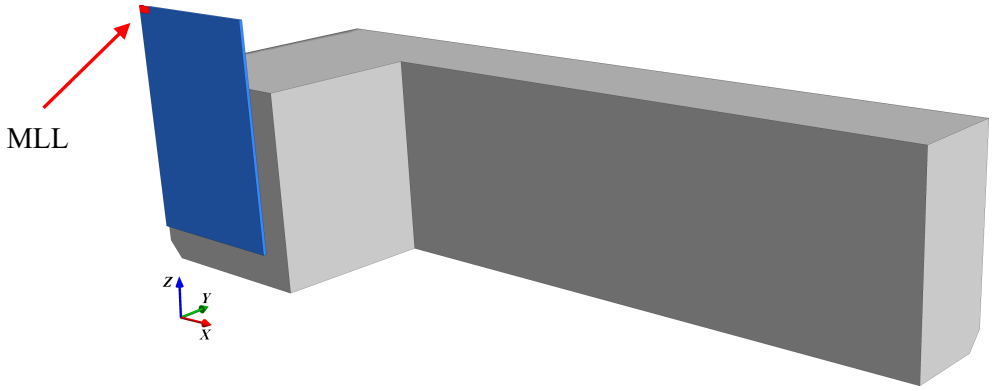

Figure 1. Geometric model. The X-ray beam is parallel to the y-coordinate axis.

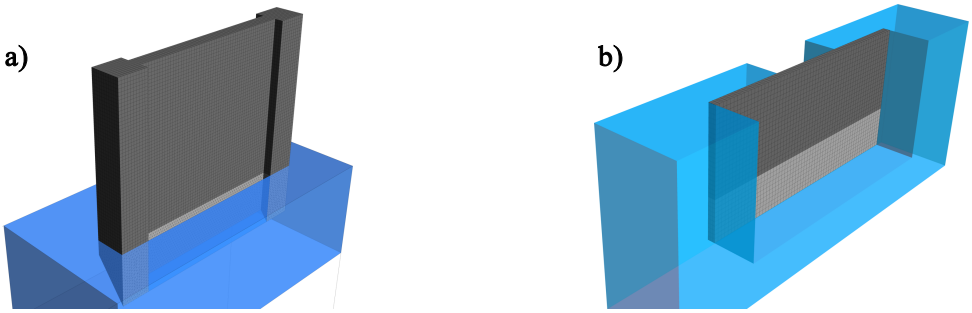

Figure 2. The MLL designs under consideration: **a)** old shape and **b)** new shape.

The MLL was attached to the top of the diamond plate (old design used in European XFEL experiment) as shown in figure 2 (left image). In the new mounting geometry shown on the right (figure 2) the XFEL beam is assumed to illuminate only the free-standing part of the MLL (where there is a window in diamond plate), while in the areas on both sides of this window the lens is in contact to the diamond plate. This design anticipated faster heat dissipation from the MLL to the diamond, which is a good thermal conductor. The optical thickness of the lenses (thickness in the X-ray propagation direction) used in numerical simulations was chosen as that which gives the maximum diffraction efficiency for an ideal multilayer structure.

Due to the significant difference in the dimensions of the holder (cm-scale), plate (mm-scale), and lens (μm-scale), each part was meshed separately. Because these parts have different cell sizes, a non-conformal mesh interface was used to assemble the final computational mesh. The MLL computational mesh can be seen in figure 2. The silicon substrate (light gray) was included in the model and numerical simulations. The simulation assumed that the lenses were in air (as in the European XFEL experiment).

Instead of simulating ten thousand layers in the structure of the MLL, the model replaced this with a structure of the same overall size as the MLL that consisted of a weighted average of the materials according to the material ratios listed in table 1.

First, we performed a grid sensitivity study [10]. For this purpose, coarse, medium, and fine MLL grids with 2100, 16800, and 134400 cells were used. We found that the results for the medium and fine grids were very similar. Therefore, further numerical simulations were carried out with the medium grid due to its lower computational requirements.

2.3. Material Properties and Boundary Conditions

Table 1 summarizes the properties of the materials used in the numerical simulations. In addition to the WC/SiC multilayer, which was used in aforementioned European XFEL, we also evaluated the performance of two additional multilayer material pairs (Ti/SiC and TiC/SiC), which were selected based on their potential to form good quality multilayers, and their low densities and high melting temperatures. With one exception, an equal amount of both materials in each multilayer period was considered. For the TiC/SiC multilayer we also simulated the case of a ratio of 30% TiC to 70% SiC. Due to the lack of reliable data on the temperature dependence of some material properties (especially emissivity), constant values were used in the simulations.

Table 1. Bulk material properties of materials and multilayer material pairs.

Domain	Material	ρ (kg m^{-3})	k (W m^{-1} K^{-1})	c_p (J kg^{-1} K^{-1})	ε
holder	aluminum (Al)	2719	202	871	0.4
plate	diamond (C)	3500	2000	510	0.6
substrate	silicon (Si)	2329	105	785	0.5
multilayer	50 % WC – 50 % SiC	8450	115	476	0.5
	50 % TiC – 50 % SiC	4015	75	815	0.7
	30 % TiC – 70 % SiC	3649	93	789	0.7
	30 % Ti – 70 % SiC	3529	91	690	0.6

To solve equation (1), the combined external convection and radiation thermal boundary conditions were used. The following equation gives the wall heat flux

$$-k\frac{\partial T}{\partial n} = \alpha\left(T - T_\infty\right) + \varepsilon\sigma\left(T^4 - T_\infty^4\right), \tag{3}$$

where σ = 5.67×10^{-8} W m^{-2} K^{-4} is the Stefan-Boltzmann constant, α = 20 W m^{-2} K^{-1} is the heat transfer coefficient, ε is surface emissivity (table 1) and T_∞ = 296 K is the ambient temperature.

3. Results

3.1. Lens shape

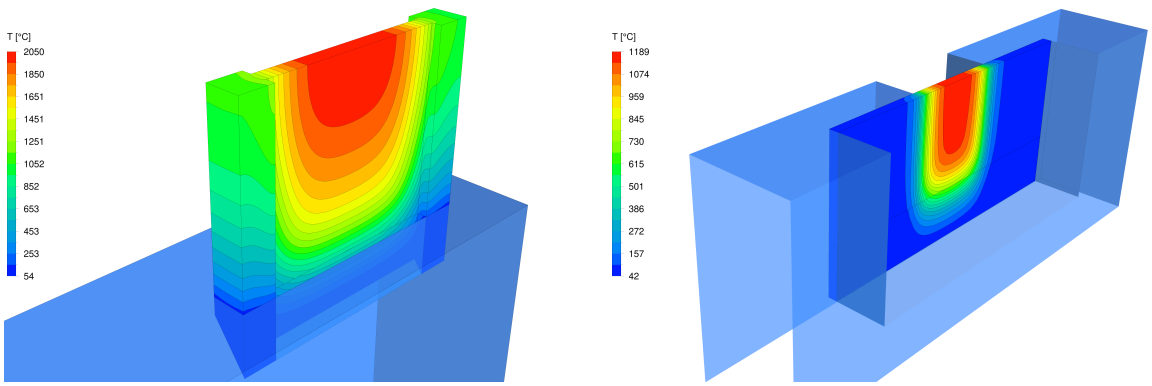

Figure 3. MLL surface temperature for the old and new lens mounting.

In figure 3 we compare temperature distributions of the old and new lens mounting (see also figure 2) for the WC/SiC multilayer and a pulse frequency of 10 kHz. It is assumed that the multilayer consists of 50% WC (T_{melt} = 2807 °C) and 50% SiC (T_{melt} = 2830 °C). The optimal lens thickness for this material ratio at a photon energy of 17.5 keV is d_{opt} = 9 µm. For an incident pulse energy of 1 mJ the absorbed energy for this thickness is Q_{abs} = 376 mJ. In the old design (using the above parameters) the temperature in the lens reached 2050 °C. According to our simulations, the maximum temperature in the new design dropped by almost half to 1187 °C. Numerical simulations confirmed that a large MLL–diamond plate contact area substantially increased the heat dissipation from the lens and this design is better than the old one, but the maximum temperature is probably still too high to prevent de-attachment.

3.2. Ratio of multilayer materials

Another important parameter that can be tuned in MLLs is the material used in the multilayer structure. A multilayer pair consists of two materials. Their ratio determines the optimum lens thickness and thus the absorbed energy and the temperature load on the lens. Figure 4 shows the development of the peak temperature as a function of time in MLLs consisting of TiC and SiC layers. This material pair was studied as an alternative to WC/SiC [7]. The simulations assumed TiC/SiC-based MLL mounted using a new lens design (figure 3, right image) and exposed to pulse frequency of 10 kHz. The simulation results predict dramatic decrease in maximum temperature. As shown, a lower amount of higher density material (TiC) in the multilayer (30% TiC – 70% SiC) is more favorable, even though the optical thickness is higher.

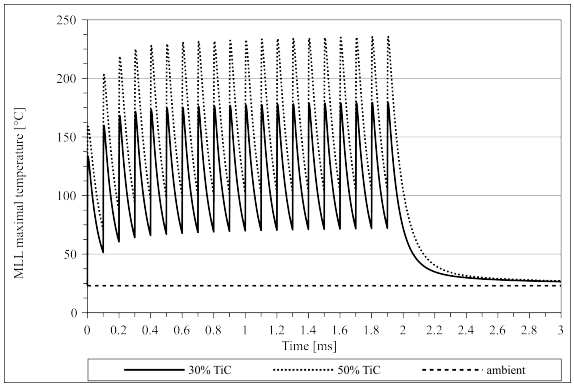

Figure 4. Evolution of the maximum temperature for two different material ratios of TiC/SiC-based MLL as the lens is exposed to 20 XFEL pulses at 1 mJ pulse energy. Solid line: 30% TiC – 70% SiC (d_{opt} = 62 µm, Q_{abs} = 198 mJ). Dotted line: 50% TiC – 50% SiC (d_{opt} = 50 µm, Q_{abs} = 223 mJ). The maximum temperatures of the lens are 179.5 °C and 235.5 °C, respectively. The melting temperature for TiC is 3160 °C and 2830 °C for SiC.

3.3. X-ray pulse frequency

The frequency of the XFEL pulses has a significant influence on the lens temperature. Figure 5 compares the peak temperatures of the Ti/SiC-based MLL mounted using the new lens design, exposed to 10 kHz and 278 kHz XFEL pulse frequency, respectively.

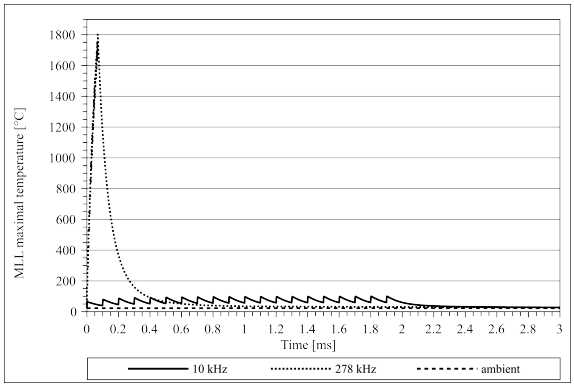

Figure 5. Evolution of maximum temperature in Ti/SiC-based MLL (30% Ti – 70% SiC, d_{opt} = 86 µm, Q_{abs} = 280 mJ) for pulse frequency of 10 kHz and 278 kHz. For 278 kHz pulse frequency the maximum temperature in the lens reaches T_{max} = 1802 °C while for 10 kHz it is T_{max} = 216.8 °C. The melting temperature for Ti is 1941 °C and 2830 °C for SiC.

At higher pulse frequencies, the temperature rises sharply (in less than 0.2 ms) approaching the melting temperature of titanium. Since the interval between successive pulses in this simulated case is very short, the lens cannot cool down before the next pulse. At lower frequencies the lens temperature drops significantly due to cooling so that after the last pulse, the maximum temperature is much lower than the melting temperature of titanium. These results suggest that Ti/SiC-based MLLs could be used for focusing XFEL beams with 10 kHz pulse frequency but is not suitable for pulse frequency of 278 kHz or higher.

4. Conclusions

After creating the geometric model, generating the computational mesh, determining the material properties, and applying the boundary conditions, we performed a mesh sensitivity study. Temperature distributions inside the MLL after exposure to 20 XFEL pulses were calculated. We examined how the temperature varies as a function of pulse frequency and investigated the heating of MLLs composed of different material pairs including WC/SiC, Ti/SiC and TiC/SiC.

Our simulations show that the lens heats up instantaneously and that the heat dissipates into the environment through radiation and convection. With each successive pulse, the temperature of the lens rises again. For XFEL experiments with pulse frequencies >10 Hz the temperature in the lenses rises sharply, and significant temperature stresses can occur. This is undesirable as the lens deforms and it may no longer satisfy the Bragg condition.

In conclusion, we demonstrated that the numerical simulations are a very efficient way of studying systems with complex geometries and boundary conditions where analytical solutions are not feasible. Here, they provided an insight and better understanding of the heat transfer process and thermal loads on MLLs exposed to XFEL beams as a function of pulse frequency, different materials and mounting geometries. Numerical simulations helped to select the most heat transfer efficient lens geometry and substantially reduced the time and cost to analyze the suitability of different materials based on their thermal properties. These results are very valuable and will be used for designing new MLLs for future XFEL experiments.

References

[1] Bajt S, Prasciolu M, Fleckenstein H et al 2018 *Light: Sci. Appl.* X-ray focusing with efficient high-NA multilayer Laue lenses **7** e17162

[2] Morgan AJ, Murray KT, Prasciolu M et al 2020 *J. Appl. Cryst.* **53** 927-936

[3] Li T, Dresselhaus JL, Ivanov N et al 2023 *Light: Science & Applications **12** 130*

[4] Prasciolu M, Murray KT, Ivanov N et al 2021 *Int. Conf. on X-ray Lasers* vol 11886 ed D Bleiner (Bellingham: SPIE) p 11860M

[5] Prasciolu M, Murray KT, Ivanov N et al 2022 "On the use of multilayer Laue lenses with X-ray Free Electron Lasers" arXiv:2203.11712

[6] Prasciolu M and Bajt S 2018 *Appl. Sci.* **8** 571

[7] Rek Z, Chapman HN, Šarler B and Bajt S 2022 *Photonics* Numerical Simulation of Heat Load for Multilayer Laue Lens under Exposure to XFEL Pulse Trains **202** 9(5):362

[8] ANSYS® Academic research CFD Release 18.2.

[9] Incropera F and DeWitt D 2002 *Fundamentals of Heat and Mass Transfer* (New York: John Wiley & Sons)

[10] Roache PJ 1998 *Verification and Validation in Computational Science and Engineering* (Albuquerque: Hermosa)